Int. J. Heat Mass Transfer. Vol. 18, pp. 227–236. Pergamon Press 1975. Printed in Great Britain

FINITE ELEMENT ANALYSIS OF LAMINAR CONVECTIVE HEAT TRANSFER IN VERTICAL DUCTS WITH ARBITRARY CROSS-SECTIONS

A. L. NAYAK† and PING CHENG‡
Department of Mechanical Engineering, University of Hawaii, Honolulu, Hawaii 96822

(*Received* 2 *February* 1973 *and in revised form* 1 *July* 1974)

Abstract—The problem of combined free and forced convection, in a fully developed laminar steady flow through vertical ducts under the conditions of constant axial heat flux and uniform peripheral wall temperature, is considered. Finite element solution algorithm with triangular elements and piecewise linear interpolation polynomials for temperature and velocity profiles are derived for ducts with arbitrary shape. Numerical values for Nusselt numbers at selected Rayleigh numbers are obtained for the special cases of square and triangular ducts.

NOMENCLATURE

A, cross-sectional area of the duct;
a_1^e, a_2^e, a_3^e, constants in equation (12);
$\{B\}$, global column matrix defined by equation (26b);
$\{B^e\}$, nodal column matrix defined by equation (23b);
C, axial temperature gradient;
C_p, specific heat at constant pressure;
c_1^e, c_2^e, c_3^e, constants in equation (12);
$[D^e]$, displacement matrix defined by equation (21c);
$[D^e]^T$, transpose of $[D^e]$;
d, equivalent hydraulic diameter, $4A/P$;
E, total number of finite elements;
$[F^e]$, nodal matrix defined by equation (23d);
$[F]$, global matrix defined by equation (26b);
g, gravitational acceleration;
h, average peripheral heat-transfer coefficient;
i, j, k, vertices of the triangular element;
k_f, thermal conductivity of the fluid;
L, pressure gradient parameter, $-d^2[\mathrm{d}p^*/\mathrm{d}z^* + \rho_w^* g]/\mu\omega_m$;
$[M^e]$, nodal matrix defined by equation (23c);
$[M]$, global matrix defined by equation (26b);
m, dummy index;
N, total number of nodal points;
Nu, Nusselt number, hd/k_f;
n, dummy indexes;
P, perimeter of the duct;
$\{p\}$, column matrix defined by equation (14a);
$\{p\}^T$, transpose of $\{p\}$;
$[R^e]$, matrix defined by equation (14d);
Ra, Rayleigh number, $\rho^{*2} g C_p C\beta d^4/\mu k_f$;
T, temperature;
T_w, wall temperature [dimensional];
T_0, wall temperature at $z = 0$ [dimensional];
$\{T\}$, global column matrix defined by equation (18a);
$\{T^e\}$, nodal column matrix defined by equation (14c);
t, temperature difference defined by equation (4) [dimensional];
t_m, mean temperature difference defined by equation (27b) [dimensionless];
u^*, velocity in x-direction [dimensional];
V, variational integral defined by equation (11);
V^e, variational integral defined by equation (15b);
$V_\omega^e, V_t^e, V_s^e, V_c^e$, variational integrals defined by equation (22b);
v^*, velocity in y-direction [dimensional];
$\{W\}$, global column matrix defined by equation (18a);
$\{W^e\}$, nodal column matrix defined by equation (14b);
w^*, velocity in z-direction [dimensional];
w, dimensionless velocity in z-direction;
w_m^*, mean velocity [dimensional];
x^*, y^*, z^*, cartesian coordinates [dimensional];
x, y, z, dimensionless coordinates, $x = x^*/d$, $y = y^*/d$, $z = z^*/d$;
$\{\ \}$, column matrix;
$[\ ]$, matrix.

Greek symbols

α, β, γ, quantities defined in equation (14d);
μ, viscosity;
ρ^*, density [dimensional].

†Graduate student.
‡Professor.

Subscripts

0, reference point at $z = 0$;
w, on the wall.

Superscripts

*, dimensional quantities;
e, quantities associates with a particular triangular element.

INTRODUCTION

THE PROBLEM of combined free and forced convection in vertical ducts, under the conditions of constant axial heat flux and uniform peripheral wall temperature, has important applications in compact heat exchangers where design considerations may dictate ducts with unconventional shapes. Although numerous studies on this problem have been conducted both theoretically and experimentally, analytical solutions have been confined to ducts with relatively simple shapes such as rectangular [1–4], circular [5, 6], triangular [7], and polygonal [8]. For more complicated geometries, where analytical solutions are not possible, recent developments in numerical techniques suggest that it can best be handled by means of the finite element method (FEM).

In this paper, finite element solution algorithm with triangular elements and piecewise linear interpolation polynomials for temperature and velocity profiles are derived for ducts with arbitrary shape. A computer program embodying the solution algorithm has been developed. By specifying the locations of boundary and interior nodes and other parameters as input data, numerical values for Nusselt number, velocity, and temperature profiles in a duct with any shape can be obtained. For illustration: computations were carried out for a square duct; an equilateral-triangular duct; a 30–60 right-triangular duct; and a right-angled, isosceles-triangular duct. Comparison of these numerical results to those of the exact solutions shows that they are in good agreement. Comparison between finite element method and the finite difference method for a square duct is also made.

GOVERNING EQUATIONS AND BOUNDARY CONDITIONS

As in [1–8], the mathematical formulation of the problem is based on the following assumptions:

1. The fluid is assumed to be viscous and heat conducting and in a steady motion.
2. Fully developed velocity and temperature profiles are assumed.
4. Fluid properties are assumed to be constant; except the density in formulating the body-force term, where the density is linear to and varying with temperature.
4. Frictional heating due to viscosity is neglected.
5. No internal heat generation.
6. Heat input in the axial direction, i.e. in z-direction, is constant.
7. Wall temperature is uniform in the transversed $(x$–$y)$ plane.

For a fully developed incompressible laminar flow, Maslen [9] has shown that the velocities transverse to the flow are zero, namely, $u^* = v^* = 0$. Since $\partial\omega^*/\partial z^* = 0$ for a fully developed flow, the continuity equation is automatically satisfied. With $u^* = v^* = 0$, the momentum equations in the x and y directions give $\partial p^*/\partial x = \partial y^* = 0$, whereas the momentum equation in the z-direction gives

$$\mu\left(\frac{\partial^2\omega^*}{\partial x^{*2}} + \frac{\partial^2\omega^*}{\partial y^{*2}}\right) = \rho^* g + \frac{\mathrm{d}p^*}{\mathrm{d}z^*}. \tag{1}$$

With the conditions $u^* = v^* = 0$ and the assumptions (5) and (6), the energy equation becomes

$$k_f\left(\frac{\partial^2 T^*}{\partial x^{*2}} + \frac{\partial^2 T^*}{\partial y^{*2}} + \frac{\partial^2 T^*}{\partial z^{*2}}\right) = \rho^* C_p \omega^* \frac{\partial T^*}{\partial z^*}. \tag{2}$$

For a fully developed temperature profile and constant axial heat flux, Seban and Shimazaki [10] have shown that $\partial T^*/\partial z^* = \partial T_w^*/\partial z^* = C$ where C is a constant. It follows that the wall temperature is given by

$$T_w^*(z^*) = T_0^* + Cz^*, \tag{3}$$

where we have also taken into consideration of assumption (7). Equation (3) suggests that the temperature distribution in the flow field is of the form

$$T^*(x^*, y^*, z^*) = T_w^*(z^*) + t^*(x^*, y^*). \tag{4}$$

Substituting equation (4) into equations (1) and (2) and assuming that the density varies linearly with temperature in the body force term, namely,

$$\rho^* = \rho_w^*[1 - \beta(T^* - T_w^*)],$$

we have

$$\mu\left(\frac{\partial^2\omega^*}{\partial x^{*2}} + \frac{\partial^2\omega^*}{\partial y^{*2}}\right) = \frac{\partial p^*}{\partial z^*} + \rho_w^* g(1 - \beta t^*), \tag{5}$$

$$k_f\left(\frac{\partial^2 t^*}{\partial x^{*2}} + \frac{\partial^2 t^*}{\partial y^{*2}}\right) = \rho^* C_p C\omega^*. \tag{6}$$

The boundary conditions are $t^* = \omega^* = 0$ on the wall.

As in [2, 4, 7, 8], we shall now introduce the following dimensionless variables;

$$\begin{aligned} x &= x^*/d, \qquad y = y^*/d, \\ t &= t^*/\rho^* C_p C d^2 \omega_m^*/k_f, \\ \omega &= \omega^*/\omega_m^*, \end{aligned} \tag{7}$$

where

$$\omega_m^* \equiv \frac{1}{A}\iint \omega^* \,\mathrm{d}x^* \,\mathrm{d}y^*$$

is the mean velocity in the z-direction, and $d = 4A/P$ is the equivalent diameter with A denoting the cross-sectional area and P the perimeter of the duct. Equations (5) and (6) in dimensionless form are given by

$$\frac{\partial^2\omega}{\partial x^2}+\frac{\partial^2\omega}{\partial y^2}+Ra\,t+L=0, \tag{8}$$

$$\frac{\partial^2 t}{\partial x^2}+\frac{\partial^2 t}{\partial y^2}-\omega=0, \tag{9}$$

where L and Ra are respectively the pressure gradient parameter and the Rayleigh number given by $L \equiv -d^2[\mathrm{d}p^*/\mathrm{d}z^*+\rho_W^* g]/\mu w_m^*$ and $Ra \equiv \rho^{*2} g C_p C\beta d^4/\mu k_f$. The boundary conditions in terms of dimensionless variables are

$$t=\omega=0 \text{ on the wall.} \tag{10}$$

Equations (8) and (9) with boundary condition (10) are a set of coupled linear partial differential equations with homogeneous boundary conditions. It is noted that, for the case of $Ra = 0$, equations (8) and (9) are then decoupled with both the velocity and temperature fields governed by the Poisson equation but with different inhomogeneous terms. The condition of $Ra = 0$ corresponds to either $\beta = 0$ or $C = 0$. The former corresponding to the case of incompressible flow where no free convection occurs; the latter corresponding to the case where wall temperature is uniform everywhere and equation (9) vanishes [3].

APPLICATIONS OF FINITE ELEMENT METHOD

For cross-sections with simple shape such as rectangular, triangular, circular or polygonal, analytical solutions to equations (8) and (9) with boundary condition (10) have been obtained. For more complicated shapes, however, analytical solutions are not possible. It is the purpose of this paper to obtain numerical solutions to ducts with arbitrary cross sections by the application of the finite element method (see [11, 12] for a general discussion of the finite element method).

Instead of dealing directly with the differential equations, the finite element method is a numerical scheme to perform the extremization of the corresponding functional. It can be shown that the solution to equations (8) and (9) with boundary conditions (10) is equivalent to extremizing the following functional [13]

$$V=\iint_A\left\{\left[\left(\frac{\partial\omega}{\partial x}\right)^2+\left(\frac{\partial\omega}{\partial y}\right)^2\right]-2\omega(L+Rat)-Ra\left[\left(\frac{\partial t}{\partial x}\right)^2+\left(\frac{\partial t}{\partial y}\right)^2\right]\right\}\mathrm{d}x\,\mathrm{d}y, \tag{11}$$

where A is the cross-sectional area of the duct.

We now subdivide the cross section of the duct into a number of "finite elements". These finite elements may take any geometric shape or size. In general, a triangular element is preferred since it has a more flexible structure enabling them to approximate arbitrary region with greater fidelity. For this reason, the authors chose the triangular shape as the finite element, with vertices of the triangle as nodal points denoting by the integers, i, j and k. Within the triangular element, we assume piecewise linear interpolation polynomials for velocity and temperature distributions. Thus we have

$$\begin{aligned}\omega^e &= c_1^e+c_2^e x+c_3^e y,\\ t^e &= a_1^e+a_2^e x+a_3^e y,\end{aligned} \tag{12}$$

where c_m^e and a_m^e $(m = 1, 2, 3)$ are constants to be expressed in terms of $\omega_i, \omega_j, \omega_k, t_i, t_j, t_k$ which are the values of ω and t at the vertices located at (x_i, y_i), (x_j, y_j) and (x_k, y_k). Imposing (12) on the nodal values at the vertices of the triangular element, equation (12) can be written in the following matrix form

$$\begin{aligned}\omega^e &= \{p\}^T[R^e]\{W^e\},\\ t^e &= \{p\}^T[R^e]\{T^e\},\end{aligned} \tag{13}$$

where $\{p\}$, $\{W^e\}$, and $\{T^e\}$ are column matrix given by

$$\{p\}=\begin{Bmatrix}1\\ x\\ y\end{Bmatrix}, \tag{14a}$$

$$\{W^e\}=\begin{Bmatrix}\omega_i\\ \omega_j\\ \omega_k\end{Bmatrix}, \tag{14b}$$

$$\{T^e\}=\begin{Bmatrix}t_i\\ t_j\\ t_k\end{Bmatrix}, \tag{14c}$$

and

$$[R^e]=\frac{1}{2A^e}\begin{bmatrix}\alpha_p & \alpha_q & \alpha_r\\ \beta_p & \beta_q & \beta_r\\ \gamma_p & \gamma_q & \gamma_r\end{bmatrix}, \tag{14d}$$

where $A^e \equiv \frac{1}{2}|x_{ij}y_{jk}-x_{jk}y_{ij}|$ is the area of the triangular element and $x_{ij} \equiv x_j-x_i, y_{jk} \equiv y_k-y_j, \alpha_p \equiv x_q y_r-x_r y_q$, $\beta_p \equiv y_q-y_r$, $\gamma_p \equiv x_r-x_q$ with the indices (p, q, r) permute cyclicly in the order (i, j, k).

We now break up the integral (11) into E elements. Thus, we have

$$V=\sum_{e=1}^{E} V^e, \tag{15a}$$

where

$$V^e \equiv \iint_{A^e} \left\{ \left[\left(\frac{\partial \omega^e}{\partial x} \right)^2 + \left(\frac{\partial \omega^e}{\partial y} \right)^2 \right] - 2\omega^e (L + Rat^e) - Ra \left[\left(\frac{\partial t^e}{\partial x} \right)^2 + \left(\frac{\partial t^e}{\partial y} \right)^2 \right] \right\} dx\, dy. \quad (15b)$$

Substituting equations (13) into equations (15) and performing the integration, we have

$$V^e = f_1(\omega_i, \omega_j, \omega_k, t_i, t_j, t_k), \quad (16a)$$

and

$$V = \sum_{e=1}^{E} V^e = f_2(\omega_1, \omega_2, \ldots, \omega_N, t_1, t_2, \ldots, t_N), \quad (16b)$$

where the subscript N denotes the total number of nodes in the cross-section. Because the required nodal values of temperature and velocity are those that extremize V, the unknown nodal values must satisfy the set of linear algebraic equations given

$$\begin{Bmatrix} \frac{\partial V}{\partial \omega_1} \\ \frac{\partial V}{\partial \omega_2} \\ \cdot \\ \cdot \\ \cdot \\ \frac{\partial V}{\partial \omega_N} \\ \frac{\partial V}{\partial t_1} \\ \frac{\partial V}{\partial t_2} \\ \cdot \\ \cdot \\ \cdot \\ \frac{\partial V}{\partial t_N} \end{Bmatrix} = \{0\}. \quad (17)$$

Now, if we denote the global column vectors $\{W\}$ and $\{T\}$ by

$$\{W\} \equiv \begin{Bmatrix} \omega_1 \\ \omega_2 \\ \cdot \\ \cdot \\ \cdot \\ \omega_N \end{Bmatrix}, \quad \{T\} \equiv \begin{Bmatrix} t_1 \\ t_2 \\ \cdot \\ \cdot \\ \cdot \\ t_N \end{Bmatrix}, \quad (18a)$$

and

$$\left\{ \frac{\partial V}{\partial W} \right\} \equiv \begin{Bmatrix} \frac{\partial V}{\partial \omega_1} \\ \frac{\partial V}{\partial \omega_2} \\ \cdot \\ \cdot \\ \cdot \\ \frac{\partial V}{\partial \omega_N} \end{Bmatrix}, \quad \left\{ \frac{\partial V}{\partial T} \right\} \equiv \begin{Bmatrix} \frac{\partial V}{\partial t_1} \\ \frac{\partial V}{\partial t_2} \\ \cdot \\ \cdot \\ \cdot \\ \frac{\partial V}{\partial t_N} \end{Bmatrix}, \quad (18b)$$

then equation (17) can be rewritten as

$$\begin{Bmatrix} \frac{\partial V}{\partial W} \\ \frac{\partial V}{\partial T} \end{Bmatrix} = \{0\}, \quad (19a)$$

where

$$\left\{ \frac{\partial V}{\partial W} \right\} = \left\{ \frac{\partial}{\partial W} \sum_{e=1}^{E} V^e \right\} = \left\{ \sum_{e=1}^{E} \frac{\partial V^e}{\partial W} \right\},$$

$$\text{and} \quad \left\{ \frac{\partial V}{\partial T} \right\} = \left\{ \frac{\partial}{\partial T} \sum_{e=1}^{E} V^e \right\} = \left\{ \sum_{e=1}^{E} \frac{\partial V^e}{\partial T} \right\}. \quad (19b)$$

The derivatives of V^e with respect to $\{W\}$ and $\{T\}$ in equation (19b) is a column matrix that is mostly zero because V^e depends only on ω_i, ω_j, ω_k, and t_i, t_j, and t_k as given by equation (16a). It follows that

$$\left\{ \frac{\partial V^e}{\partial W} \right\} = \begin{Bmatrix} 0 \\ \cdot \\ \cdot \\ \cdot \\ \frac{\partial V^e}{\partial \omega_i} \\ \cdot \\ \cdot \\ \frac{\partial V^e}{\partial \omega_j} \\ \cdot \\ \cdot \\ \frac{\partial V^e}{\partial \omega_k} \end{Bmatrix} \begin{matrix} \\ \\ \\ \\ \text{-}i\text{th row} \\ \\ \\ \text{-}j\text{th row,} \\ \\ \\ \text{-}k\text{th row} \end{matrix}$$

$$\text{and} \quad \left\{\frac{\partial V^e}{\partial T}\right\} = \begin{Bmatrix} 0 \\ \cdot \\ \cdot \\ \cdot \\ \dfrac{\partial V^e}{\partial t_i} \\ \cdot \\ \cdot \\ \dfrac{\partial V^e}{\partial t_j} \\ \cdot \\ \cdot \\ \dfrac{\partial V^e}{\partial t_k} \end{Bmatrix} \begin{matrix} \\ \\ \\ \\ \text{-}i\text{th row} \\ \\ \\ \text{-}j\text{th row}, \\ \\ \\ \text{-}k\text{th row} \end{matrix} \tag{20}$$

where the position of the non-vanishing coefficients vary from element to element since the values of i, j, and k are different for each element. As suggested by Myers [12], it will be convenient to rewrite the above column matrix as

$$\left\{\frac{\partial V^e}{\partial W}\right\} = [D^e]\left\{\frac{\partial V^e}{\partial W^e}\right\} \quad \text{and} \quad \left\{\frac{\partial V^e}{\partial T}\right\} = [D^e]\left\{\frac{\partial V^e}{\partial T^e}\right\}, \tag{21a}$$

where

$$\left\{\frac{\partial V^e}{\partial W^e}\right\} \equiv \begin{Bmatrix} \dfrac{\partial V^e}{\partial \omega_i} \\ \dfrac{\partial V^e}{\partial \omega_j} \\ \dfrac{\partial V^e}{\partial \omega_k} \end{Bmatrix}, \qquad \left\{\frac{\partial V^e}{\partial T^e}\right\} \equiv \begin{Bmatrix} \dfrac{\partial V^e}{\partial t_i} \\ \dfrac{\partial V^e}{\partial t_j} \\ \dfrac{\partial V^e}{\partial t_k} \end{Bmatrix}, \tag{21b}$$

and $[D^e]$ is the displacement matrix given by

$$[D^e] \equiv \begin{bmatrix} 0 & 0 & 0 \\ 1 & 0 & 0 \\ 0 & 0 & 0 \\ \cdot & \cdot & \cdot \\ \cdot & \cdot & \cdot \\ 0 & 1 & 0 \\ \cdot & \cdot & \cdot \\ \cdot & \cdot & \cdot \\ 0 & 0 & 1 \\ \cdot & \cdot & \cdot \\ \cdot & \cdot & \cdot \\ 0 & 0 & 0 \end{bmatrix} \begin{matrix} \\ \text{-}i\text{th row} \\ \\ \\ \\ \text{-}j\text{th row} \\ \\ \\ \text{-}k\text{th row}, \\ \\ \\ \end{matrix} \tag{21c}$$

which is a $N \times 3$ matrix with the location of non-vanishing coefficients varying from element to element.

To obtain the explicit expressions for $\{\partial V^e/\partial W^e\}$ and $\{\partial V^e/\partial T^e\}$, it is convenient to consider the integral (15b) in several parts by writing it as

$$V^e(\omega_i, \omega_j, \omega_k, t_i, t_j, t_k) = V^e_\omega + V^e_t + V^e_s + V^e_c, \tag{22a}$$

where

$$\begin{aligned} V^e_w(\omega_i, \omega_j, \omega_k) &\equiv \iint_{A^e} \left[\left(\frac{\partial \omega^e}{\partial x}\right)^2 + \left(\frac{\partial \omega^e}{\partial y}\right)^2\right] dx\, dy, \\ V^e_t(t_i, t_j, t_k) &\equiv \iint_{A^e} \left[\left(\frac{\partial t^e}{\partial x}\right)^2 + \left(\frac{\partial t^e}{\partial y}\right)^2\right] dx\, dy, \\ V^e_s(\omega_i, \omega_j, \omega_k) &\equiv 2 \iint_{A^e} L\omega^e\, dx\, dy, \\ V^e_c(\omega_i, \omega_j, \omega_k, t_i, t_j, t_k) &\equiv -2 \iint_{A^e} Ra\omega^e t^e\, dx\, dy. \end{aligned} \tag{22b}$$

Substituting equation (13) into equations (22b) and differentiating, it can be shown that

$$\begin{aligned} \left\{\frac{\partial V^e_\omega}{\partial W^e}\right\} &= [F^e]\{W^e\}, \\ \left\{\frac{\partial V^e_t}{\partial W^e}\right\} &= \{0\}, \\ \left\{\frac{\partial V^e_s}{\partial W^e}\right\} &= -L\{B^e\}, \\ \left\{\frac{\partial V^e_c}{\partial W^e}\right\} &= Ra[M^e]\{T^e\}, \end{aligned} \tag{23a}$$

where

$$\{B^e\} \equiv \tfrac{2}{3}A^e \begin{Bmatrix} 1 \\ 1 \\ 1 \end{Bmatrix}, \tag{23b}$$

$$[M^e] = -\frac{A^e}{6}\begin{bmatrix} 2 & 1 & 1 \\ 1 & 2 & 1 \\ 1 & 1 & 2 \end{bmatrix}, \tag{23c}$$

$$[F^e] \equiv \frac{2A^e}{(x_{ij}y_{jk} - x_{jk}y_{ij})^2}\begin{bmatrix} f_{11} & f_{12} & f_{13} \\ & f_{22} & f_{23} \\ \text{symmetric} & & f_{33} \end{bmatrix}, \tag{23d}$$

with

$$\begin{aligned} f_{11} &\equiv (x_{jk}^2 + y_{jk}^2), \quad f_{12} \equiv -(x_{ik}x_{jk} + y_{ik}y_{jk}), \\ f_{13} &\equiv (x_{ij}x_{jk} + y_{ij}y_{jk}), \quad f_{22} \equiv x_{ik}^2 + y_{ik}^2, \\ f_{23} &\equiv -(x_{ij}x_{ik} + y_{ij}y_{ik}), \quad f_{33} \equiv (x_{ij}^2 + y_{ij}^2). \end{aligned}$$

The second matrix expression (23b) is given by Semenza *et al.* [14] and by Myers [15]. It follows from equations (19b), (21a), and (23) that

$$\left\{\frac{\partial V}{\partial W}\right\} = \sum_{e=1}^{E} [D^e][F^e]\{W^e\} - L\sum_{e=1}^{E} [D^e]\{B^e\} + Ra\sum_{e=1}^{E} [D^e][M^e]\{T^e\} = \{0\}. \tag{24a}$$

Similarly, we also have

$$\left\{\frac{\partial V}{\partial T}\right\}^{*} = L\sum_{e=1}^{E}[D^e][F^e]\{T^e\} + \sum_{e=1}^{E}[D^e][M^e]\{W^e\} = \{0\}. \quad (24b)$$

It will be helpful if we next relate the nodal temperatures and velocities at the vertices of the triangular element, namely, $\{T^e\}$ and $\{W^e\}$ to the entire set of nodal values $\{W\}$ and $\{T\}$. It can be shown that such a relation is given by [12]

$$\{W^e\} = [D^e]^T\{W\}, \quad \{T^e\} = [D^e]^T\{T\}, \quad (25)$$

where $[D^e]^T$ is the transpose of the matrix $[D^e]$.

With the aid of equations (25), equations (24) can be written as

$$[F]\{W\} + Ra[M]\{T\} = L\{B\}, \quad [M]\{W\} + L[F]\{T\} = \{0\}, \quad (26a)$$

where $[F]$ and $[M]$ are the global $N \times N$ matrix while $\{B\}$ is a global $N \times 1$ column matrix given respectively by

$$[F] = \sum_{e=1}^{E}[D^e][F^e][D^e]^T, \quad [M] = \sum_{e=1}^{E}[D^e][M^e][D^e]^T, \quad \{B\} = \sum_{e=1}^{E}[D^e]\{B^e\}. \quad (26b)$$

Equations (26a) are a set of $2N$ linear, nonhomogeneous, algebraic equations for the $2N$ unknowns $\omega_n (n = 1, 2, \ldots, N)$ and $t_n (n = 1, 2, \ldots, N)$.

Thus far, we have not imposed the boundary conditions. If we try to solve the set of algebraic equations given by equations (26a) as it is, it would be found that the determinant of the coefficients is zero. This is as it should be because the set of algebraic equations, without specifying the boundary conditions, would have an infinite set of solutions. A unique solution is obtained only after boundary conditions are specified. To impose the boundary conditions, we simply replace the equations corresponding to the differentiation with respect to boundary nodes by the equations $t_m = \omega_m = 0$, where m represents the value of the boundary nodes. The resulting set of linear algebraic equations can then be solved for the nodal values of temperature and velocity by standard subroutines.

After the nodal values of temperature and velocity are obtained, the average Nusselt number can be computed as follows. It has been shown that the average Nusselt number for fully developed flow in ducts under the condition of constant axial heat flux and uniform peripheral wall temperature is given by [16]

$$Nu = \frac{hd}{k_f} = -\frac{1}{4t_m}, \quad (27a)$$

where

$$t_m \equiv \frac{\iint \omega t \, dA}{\iint \omega \, dA}. \quad (27b)$$

To express equation (27b) in terms of nodal velocities and temperatures, we note that equation (27b) can be written as

$$t_m = \frac{\sum_{e=1}^{E}\iint_{A^e}\omega^e t^e \, dx\, dy}{\sum_{e=1}^{E}\iint_{A^e}\omega^e \, dx\, dy}. \quad (28)$$

Substitution of equation (13) into equation (28) yields

$$Nu = \frac{1}{4L}\frac{\sum_{e=1}^{E}\{W^e\}\{B^e\}}{\sum_{e=1}^{E}\{W^e\}^T[M^e]\{T^e\}}. \quad (29)$$

which can be evaluated once the nodal values of temperature and velocity have been computed.

RESULTS AND DISCUSSION

The finite element solution algorithm derived in the previous section is applicable to ducts of any shape. A computer program has been written to carry out the numerical solutions. By supplying the locations of the interior and boundary nodes, the values of i, j, and k for each element as well as the values of Ra and L, as input data to the computer program, nodal values of temperature, velocity, and Nusselt number for ducts with any cross-section can be computed. To assess the accuracy and convergence of the finite element method, computations were carried out for a square duct, an equilateral triangular duct, a right-angled isosceles duct, and a 30–60 right angle triangular duct. The results are compared with exact values which have been obtained by previous investigators.

Square ducts

The subdivision of a square duct into triangular finite elements can be done in many different ways. Three possible subdivisions of the duct are shown in Fig. 1 (with elements of equal size) and Fig. 2 (with elements of unequal size). The FEM solutions with two different subdivisions (corresponding to Fig. 1(a) and Fig. 1(b) respectively) were computed for a few selected sets of parameters Ra and L taken from [3].

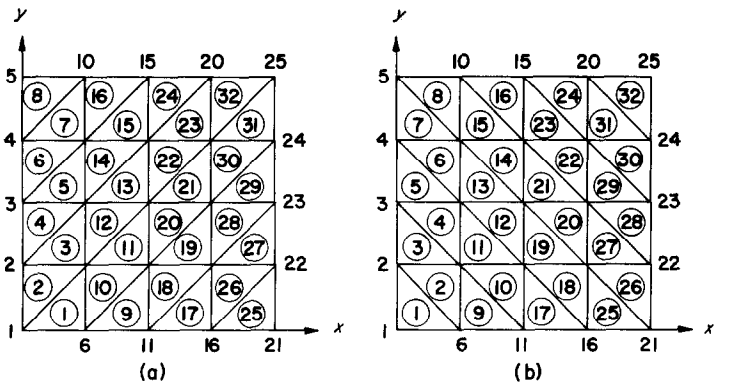

FIG. 1. Two different subdivisions (a and b) of a square duct into triangular finite elements of equal size.

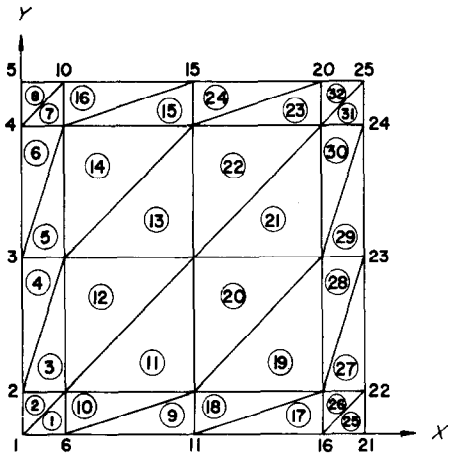

FIG. 2. Subdivision of a square duct into triangular finite elements of unequal size.

Table 1. Comparison of exact solutions and FEM solutions [with uniform mesh and discretization according to Figs. 1(a) and 1(b)] for Nusselt numbers (at various Rayleigh numbers) in a square duct.

No. of nodes	Ra = 0	π^4	$10\pi^4$	$100\pi^4$
25	4·67	4·50	4·32	6·70
81	3·85	3·87	4·30	7·60
169	3·71	3·77		7·80
Exact [3, 8]	3·61	3·69	4·27	8·27
% Error in the most accurate case	2·7	2·1	0·71	5·6

*While the exact values of Nu for other three cases are taken from Han [3], this value is obtained from [8]. We tend to agree with Iqbal *et al.* [8] that the value for this case given by Han [3] seems to be in error.

The results are then compared with the exact solution as shown in Table 1. For the present problem where boundary values are zero, the two FEM solutions give identical results.* Furthermore, the FEM solutions converge rapidly to the exact solution as more nodal points are used. For a total number of 169 nodes, the maximum error of the FEM is 5·6 per cent at $Ra = 100\pi^4$ and $L = 441{\cdot}8$.

In order to compare the FEM and FDM, numerical computations for a square duct with twenty-five nodes based on the standard five-point formula of the FDM were also carried out. It is interesting to note that, while the FEM (with triangular elements and linear interpolation polynomials) and the FDM for Poisson equation are identical to each other if both the boundary conditions and the inhomogeneous terms in the equation are independent of position, the FEM and the FDM solutions for Poisson equation are not the same if either the boundary conditions or the inhomogeneous terms is position dependent. It is for these reasons that the FEM and the FDM give identical results for velocity distribution and yet give different values for temperature distribution for the special case of $Ra = 0$ in the present problem. Comparison of the numerical results for FEM and FDM also shows that the FDM is more accurate than the FEM when a small number of nodes are used (see Table 2). In fact, while the FDM always gives symmetric results for

*If the boundary conditions depend on position, two different arrangements of triangular elements would give different results (see [12]). The authors wish to thank the reviewers for their criticism which lead to the identification of some errors in the original manuscript.

Table 2. Comparison of Nusselt numbers at various Rayleigh numbers for a square duct obtained by means of the FEM and FDM with twenty-five nodes

Methods	Ra			
	0	π^4	$10\pi^4$	$100\pi^4$
FEM	4·67	4·50	4·32	6·70
FDM	4·30	4·46	5·26	8·84
Exact [3, 8]	3·61	3·69	4·27	8·28

symmetric boundary conditions, the FEM with triangular elements and linear interpolation polynomials sometimes gives slightly unsymmetric results (actually diagonally symmetric in the present problem) for symmetric boundary conditions; its values become more and more symmetric as more nodes are used in the FEM.

One of the major advantages of the FEM is that unequal mesh size does not introduce additional complexity in the computer program. These characteristics of the FEM can be utilized with advantage by allowing greater density of elements in the critical regions where changes in the dependent variables are rapid. This consideration is desirable from the standpoint of economy, namely, it will give us more information in the critical region with less computer time than the more refined grid with uniform size. It is interesting to note that for the same number of nodes, nonuniform mesh of FEM, as in the case of FDM, will actually decrease in accuracy as indicated in Table 3.

Table 3. Nusselt numbers at various Rayleigh numbers for a square duct by means of FEM with nonuniform finite elements

No. of nodes	Ra			
	0	π^4	$10\pi^4$	$100\pi^4$
25	5·00	4·8	4·55	7·07
49	4·17	4·12	4·35	7·48
81	4·07		4·36	7·68

Triangular ducts

The computer program which was used in the calculations of square ducts can also be used for the computation of triangular ducts by supplying the locations of the boundary and interior nodes. The division scheme found to be most convenient is to draw lines parallel to all sides of the duct thus discretizing the duct in finite elements with shapes similar to the cross-section of the duct as shown in Fig. 3. Computations were carried out for an equilateral

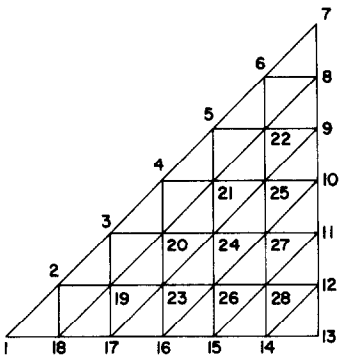

FIG. 3. Subdivision of a triangular duct into triangular finite elements of equal size.

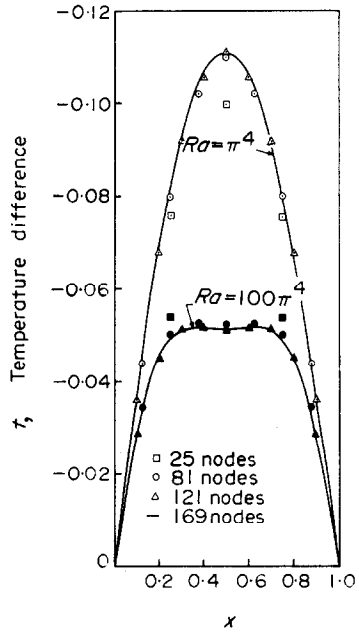

FIG. 4. Centerline temperature difference in a square duct.

triangular duct, a right-angled isosceles triangular duct, and a 30–60 right triangular duct.

Comparison of the exact values of Nusselt numbers at four different Rayleigh numbers for equilateral triangular duct obtained by Aggarwala and Iqbal [7] and that of the FEM with forty-five and ninety-one nodes are presented in Table 4. It is shown that numerical results converge to the exact values as more nodes are used. The maximum error of the FEM with ninety-one nodes is 12·3 per cent at Rayleigh number equal to 10^5. Owing to the lack of computer time, only a crude mesh of forty-five nodes was attempted

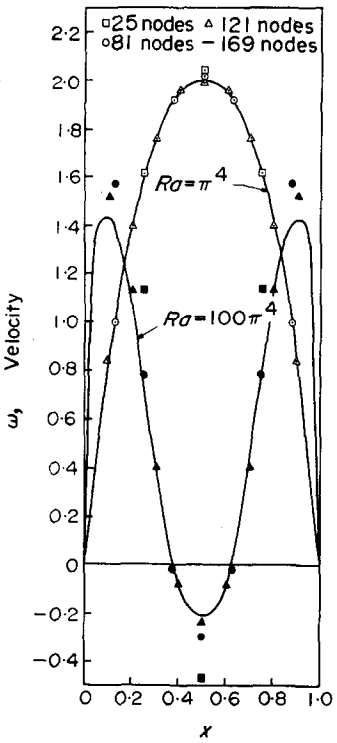

FIG. 5. Centerline velocity distribution in a square duct.

Table 4. Comparison of exact solutions and FEM solutions for Nusselt number at various Rayleigh numbers in a equilateral triangular duct

	FEM			
Ra	45 nodes	91 nodes	Exact [7]	Error (%)
0		3·22	3·11	3·6
500	3·71	3·72	3·75	0·73
20000	8·74	9·40	10·06	6·5
10^5	12·42	13·66	15·59	12·3

Table 5. Comparison of exact solutions and FEM solutions for Nusselt numbers at various Rayleigh numbers in a 30–60–90 triangular duct

Ra	FEM (45 nodes)	Exact [7]
500	3·87	3·70
2000	4·89	5·19
20000	8·79	9·97
10^5	12·39	15·21

Table 6. Comparison of exact solutions and FEM solutions for Nusselt numbers at various Rayleigh numbers in a 45–45–90 triangular duct

Ra	FEM (with 45 nodes)	Exact [7]
0	3·29	2·98
2000	4·87	5·18
20000	8·76	10·03
10^5	12·47	15·48

for the case of right-angled isosceles triangular ducts and 30–60 right triangular ducts. These numerical results along with the exact values obtained by Aggarwala and Iqbal [7] are presented in Tables 5 and 6. The agreement is good for such a crude mesh.

Acknowledgement—The first author (A.L.N.) wishes to thank Professor G. E. Myers for helpful discussions.

REFERENCES

1. S. Ostrach, Combined natural and forced convection laminar flow and heat transfer of fluids with and without heat sources in channels with linearly varying wall temperatures, N.A.C.A. TN 3141 (1954).
2. L. S. Han, Laminar heat transfer in rectangular tubes with combined free and forced convection, *J. Am. Soc. Naval Engrs* **67**, 163–167 (1955).
3. L. S. Han, Laminar heat transfer in rectangular channels, *J. Heat Transfer* **81C**, 121–127 (1959).
4. H. C. Agrawal, A variational method for combined free and forced convection in channels, *Int. J. Heat Mass Transfer* **5**, 439–444 (1962).
5. B. R. Morton, Laminar convection in uniformly heated vertical pipes, *J. Fluid Mech.* **8**, 227–240 (1960).
6. P. C. Lu, Combined free and forced convection heat generating laminar flow inside vertical pipes with circular sector cross sections, *J. Heat Transfer* **82**, 227–232 (1960).
7. B. D. Aggarawala and M. Iqbal, On limiting Nusselt numbers from membrane analogy for combined free and forced convection through vertical ducts, *Int. J. Heat Mass Transfer* **12**, 737–747 (1969).
8. M. Iqbal, S. A. Ansari and B. D. Aggarwala, Effect of buoyancy on forced convection in vertical regular polygonal ducts, *J. Heat Transfer* **92**, 237–244 (1970).
9. S. H. Maslen, Transverse velocities in fully developed flows, *Q. Appl. Math.* **16**, 173–175 (1958).
10. R. A. Seban and T. T. Shimazaki, Heat transfer to a fluid flowing turbulently in a smooth pipe with walls at constant temperature, *Trans. Am. Soc. Mech. Engrs* **73**, 803–809 (1951).
11. O. E. Zienkiewicz, *The Finite Element Method in Engineering Science*. McGraw-Hill, London (1971).
12. G. E. Myers, *Analytical Methods of Conduction Heat Transfer*. McGraw-Hill, London (1971).
13. M. Iqbal, B. D. Aggarwala and A. K. Khatry, On the conjugate problem of laminar combined free and forced convection through vertical non-circular ducts, *J. Heat Transfer* **94**, 52–56 (1972).

14. L. A. Semenza, E. E. Lewis and E. C. Rossow, Application of the finite element method to the multigroup neutron diffusion equation, *Nucl. Sci. Engng* **47**, 302–310 (1972).
15. G. E. Myers, Private communication (1972).
16. S. M. Marco and L. S. Han, A note on limiting Nusselt number in ducts with constant temperature gradient by analogy to thin-plate theory, *Trans. Am. Soc. Mech. Engrs* **77**, 625–630 (1955).

METHODE DES ELEMENTS FINIS APPLIQUEE A LA CONVECTION THERMIQUE LAMINAIRE DANS DES CONDUITES VERTICALES A SECTION DROITE ARBITRAIRE

Résumé—On considère le problème de la convection mixte pour un écoulement laminaire permanent établi dans des conduites verticales, avec des conditions de flux thermique constant et de température pariétale uniforme. L'algorithme aux éléments finis avec éléments triangulaire et interpolations polynomiales pour les profils de température et de vitesse est appliqué au cas des tubes de section droite arbitraire. On obtient les valeurs numériques des nombres de Nusselt et des nombres de Rayleigh dans le cas des conduites à sections carrée et triangulaire.

UNTERSUCHUNG DES WÄRMEÜBERGANGS BEI LAMINARER KONVEKTIONSSTRÖMUNG IN SENKRECHTEN KANÄLEN MIT WILLKÜRLICHEN QUERSCHNITTEN MITTELS DER METHODE DER FINITEN ELEMENTE

Zusammenfassung—Es wird das Problem der kombinierten freien und erzwungenen Konvektion in einer voll ausgebildeten stationären Strömung durch vertikale Kanäle mit den Bedingungen konstanten axialen Wärmestroms und einheitlicher Wandtemperatur betrachtet. Finite-Element-Lösungsalgorithmen mit Dreieckselementen und stückweisen linearen Interpolationspolynomen für Temperatur- und Geschwindigkeitsprofile werden für Kanäle mit beliebigem Querschnitt abgeleitet. Numerische Werte für Nusselt–Zahlen bei ausgewählten Rayleigh–Zahlen erhält man für die Spezialfälle der quadratischen und dreieckigen Kanäle.

АНАЛИЗ КОНВЕКТИВНОГО ТЕПЛООБМЕНА ПРИ ЛАМИНАРНОМ ТЕЧЕНИИ В ВЕРТИКАЛЬНЫХ КАНАЛАХ ПРОИЗВОЛЬНОГО СЕЧЕНИЯ МЕТОДОМ КОНЕЧНЫХ ЭЛЕМЕНТОВ

Аннотация — В работе рассматривается проблема совместной свободной и вынужденной конвекции при полностью развитом ламинарном установившемся течении в вертикальных каналах при постоянном осевом тепловом потоке и однородной температуре стенки на периферии. Для каналов произвольной формы получен алгоритм решения методом конечных элементов с треугольными элементами и кусочными линейными интерполяционными полиномами для профилей скорости и температуры. Для частных случаев квадратных и треугольных каналов получены значения чисел Нуссельта при выбранных числах Релея.